

Few-shot Algorithm Assurance

Dang Nguyen, Sunil Gupta

Applied Artificial Intelligence Institute (A²I²), Deakin University, Geelong, Australia
 {d.nguyen, sunil.gupta}@deakin.edu.au

Abstract

In image classification tasks, deep learning models are vulnerable to image distortion. For successful deployment, it is important to identify distortion levels under which the model is usable i.e. its accuracy stays above a stipulated threshold. We refer to this problem as *Model Assurance under Image Distortion*, and formulate it as a classification task. Given a distortion level, our goal is to predict if the model’s accuracy on the set of distorted images is greater than a threshold. We propose a novel classifier based on a *Level Set Estimation (LSE)* algorithm, which uses the LSE’s mean and variance functions to form the classification rule. We further extend our method to a “few sample” setting where we can only acquire few real images to perform the model assurance process. Our idea is to generate extra synthetic images using a novel *Conditional Variational Autoencoder* model with two new loss functions. We conduct extensive experiments to show that our classification method significantly outperforms strong baselines on five benchmark image datasets.

1. Introduction

Deep learning models are being increasingly developed and sold by many AI companies for decision making tasks in diverse domains. They are often trained with data usually collected under uncontrolled settings and may have imperfections e.g. noise, bias. The training process may be imperfect due to various constraints e.g. limited time-budget, small hardware. Finally, the trained models can be deployed in diverse conditions e.g. different views, at different scales, different environmental conditions, and not all of them are appropriately represented in the training data. Therefore, *at the customer side, it is important to verify/assure if the deep models work as intended, especially in scenarios where they are deployed in crucial applications.*

Assurance can be general or specific to a goal. In this paper, we want to assure if an image classifier is “accurate” under various image distortions e.g. different views, lighting conditions, etc. The reason is that image classi-

fiers often perform poorly under image distortion [20]. As an example, a ResNet-20 model [11] trained on CIFAR-10, achieves 91.37% accuracy on a validation set. When this model is deployed in practice, the input images are not always upright like the original training images, but can be slightly rotated due to an unstable camera. In this case, the model’s performance can significantly degrade. As shown in Figure 1, the model predicts wrong labels for 20-degree rotated images although these images are easily recognized by humans. The distorted images are more challenging for the model to classify them correctly, leading to an accuracy drop in 10%. The same problem can also happen when the model was trained with daylight images but deployed in night-time where the input images are often darker. Thus, *it is important for end-users to identify the distortion levels under which their purchased model is usable i.e. its accuracy stays above a stipulated threshold.*

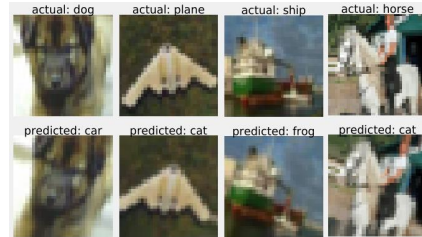


Figure 1. Model misclassifies images rotated by 20°.

We refer to the above problem as *Model Assurance under Image Distortion (MAID)*, and form it as a binary classification task. Assume that we have a pre-trained deep model T and a set of labeled images \mathcal{D} (we call it *assurance set*). We define *the search space of distortion levels* \mathcal{C} as follows: (1) each dimension of \mathcal{C} is a *type of distortion* (e.g. rotation, brightness) and (2) each point $c \in \mathcal{C}$ is a *distortion level* (e.g. {rotation=10, brightness=1.2}), which is used to modify the images in \mathcal{D} to create a set of distorted images \mathcal{D}'_c . Our goal is to learn a binary classifier that receives a distortion level $c \in \mathcal{C}$ as input and predicts if the model’s accuracy on \mathcal{D}'_c is greater than a threshold h . For example, given $h = 85\%$, $c = \{\text{rotation}=10, \text{brightness}=1.2\}$ (i.e. it rotates the images 10° and brightens them by 20%) will be classified

as “1” (“positive”) if T achieves an accuracy $a \geq 85\%$ on \mathcal{D}'_c . Otherwise, c will be classified as “0” (“negative”).

To train the classifier, we require a training set. One way to construct the training set is to randomly sample distortion level c_i from the search space \mathcal{C} , and then compute the accuracy a_i of the model T on the set of distorted images \mathcal{D}'_{c_i} . If $a_i \geq h$, we assign a label “1”. Otherwise, we assign a label “0”. Finally, we obtain the training set $\mathcal{R} = \{c_i, \mathbb{I}_{a_i \geq h}\}_{i=1}^I$, where $\mathbb{I}_{a_i \geq h}$ is an indicator function and I is the sampling budget. We then use \mathcal{R} to train a machine learning classifier e.g. neural network. However, using random distortion levels to construct the training set \mathcal{R} is not effective as often a majority of the distortion levels lead to low accuracy and thus falling under “negative” class. This leads to an *unbalanced* training set and a “one-sided” *inaccurate* classifier.

To address the above challenge, we propose a novel classifier based on the *Level Set Estimation* (LSE) algorithm [5]. First, we consider the mapping from a distortion level c to the model’s accuracy on the set of distorted images \mathcal{D}'_c as a *black-box, expensive function* $f : \mathcal{C} \rightarrow [0, 1]$. The function f is black-box as we do not know its expression, and f is expensive as we have to measure the model’s accuracy over all distorted images in \mathcal{D}'_c . Second, we approximate f using a Gaussian process (GP) [26] that is a popular method to model black-box, expensive functions. Third, we use f ’s predictive distribution in an acquisition function to search for distortion levels to update the GP. As we focus on sampling distortion levels whose predictive function values are close to the threshold, we have more chance to obtain “positive” samples. Finally, we use the mean and variance returned by the GP to form a classification rule to predict the label for any point in the search space \mathcal{C} .

We further extend our method to “*few sample*” setting where only *few original images* are available in \mathcal{D} (equivalently, we can acquire only *few distorted images*). Given a distortion level c , we typically need lots of distorted images to accurately estimate the model T ’s accuracy a on \mathcal{D}'_c . Otherwise, a can be inaccurate, which can be potentially dangerous in the context of model assurance. For example, the model may achieve 100% accuracy on 10 distorted images but its true accuracy on a large set of images at the same distortion level may be lower than the stipulated threshold. As a result, c may be inaccurately classified as “positive” while in truth its label is “negative”. As collecting a large number of images is infeasible in some domains e.g. medical or satellite images, *model assurance with few images is an important, yet challenging problem*.

To solve this problem, we try to expand the assurance set \mathcal{D} with extra synthetic images. In particular, we introduce two new losses (*distribution* and *prediction losses*) in a Conditional Variational Autoencoder (CVAE) model [27] to adapt it to our purpose. The distribution loss tries to match the distribution of the generated images with that of the

training images of the model T . We note that T ’s training images are usually inaccessible (e.g. due to privacy concern). The prediction loss tries to generate images that are recognizable by the model T . Using these losses, our generated images are more diverse and natural, which allows our LSE-based classifier to be more accurate.

To summarize, we make the following contributions.

- (1) We address the problem *Model Assurance under Image Distortion* (MAID), by proposing a LSE-based classifier to predict if the model is usable against image distortion.
- (2) We further extend our method to a “*few sample*” setting, by developing a novel generative model to synthesize high-quality and diverse images.
- (3) We extensively evaluate our method on five benchmark image datasets, and compare it with strong baselines. Our method is significantly better than other methods.
- (4) The significance of our work lies in providing ability to assure *any* image classifier T under a variety of distortions. Our method can work irrespective of whether or not T is able to provide any uncertainty in its decisions.

2. Related Background

Image distortion. Most deep learning models are sensitive to image distortion, where a small amount of distortion can severely reduce their performance. Many methods have been proposed to detect and correct the distortion in the input images [1, 20], which can be categorized into two groups: non-reference and full-reference. The non-reference methods corrected the distortion without any direct comparison between the original and distorted images [18, 4]. Other works developed models that were robust to image distortion, where most of them fine-tuned the pre-trained models on a pre-defined set of distorted images [35, 7, 14]. While these methods focused on the space of individual images to improve the model’s robustness, our work focuses on efficiently finding out the distortions where a model does not meet a required accuracy level. EXP3BO [8] used Bayesian optimization to verify a model’s performance against image distortion. It however only focused on finding the worst-case performance of the model and assumed availability of a large assurance set. In contrast, our method develops a classifier that predicts whether the model’s performance is good or bad at any distortion level in the distortion space and can work effectively even with a small assurance set.

Level set estimation (LSE). It aims to find the region where the value of a function is higher or lower than a given threshold [5]. It has many real-world applications, including environment monitor, quality control, and biotechnology [5, 3, 15]. LSE was also extended to complex problems e.g. composite functions [6], implicit problems [9], uncertain inputs [16], and high-dimensional inputs [10]. *However, there is no work applying LSE to the context of model*

assurance under image distortion.

Learning with few samples. Machine learning models often require many training samples to achieve a good accuracy, a condition that is rarely met in practice. Few samples learning (FSL) was proposed to address this problem [32]. Given a small set of training images, FSL aims to generate synthetic images to expand the training set, which helps the model to improve its generalization and performance. Several common ways to synthesize images include MixUp [31], CVAE [33], and CGAN [21], which mainly solve supervised learning problems. *We are the first to tackle the “few sample” setting for the model assurance problem.*

3. The Proposed Framework

3.1. Model assurance under image distortion

Let T be a pre-trained deep model (note that T 's training set is not accessible), $\mathcal{D} = \{x_i, y_i\}_{i=1}^N$ be a set of labeled images (i.e. *assurance set*), and $\mathcal{S} = \{S_1, \dots, S_d\}$ be a set of image distortions e.g. rotation, scale, brightness. Each S_i has a value range $[l_{S_i}, u_{S_i}]$, where l_{S_i} and u_{S_i} are the lower and upper bounds. We define a compact subset \mathcal{C} of \mathbb{R}^d as a set of all possible values for image distortion (i.e. \mathcal{C} is the search space of all possible distortion levels).

Problem statement. We consider a black-box expensive function $f: \mathcal{C} \rightarrow [0, 1]$. The function $f(c)$ receives a distortion level c as input and returns the model's accuracy on the set of distorted images $\mathcal{D}'_c = \{x'_i, y_i\}_{i=1}^N$ as output. Here, each image $x'_i \in \mathcal{D}'_c$ is a distorted version of an original image $x_i \in \mathcal{D}$. Our goal is to classify all samples in \mathcal{C} into “positive” and “negative” samples based on a user-defined threshold $h \in [0, 1]$. More precisely, given $\forall c \in \mathcal{C}$, we will assign a “positive” label to c if $f(c) \geq h$. Otherwise, c will be assigned a “negative” label. We refer this problem as *Model Assurance under Image Distortion* (MAID).

As discussed earlier, to address the MAID problem, we can train a classifier using $\mathcal{R} = \{c_i, \mathbb{1}_{f(c_i) \geq h}\}_{i=1}^I$, where c_i is randomly sampled from \mathcal{C} and I is the sampling budget. However, \mathcal{R} is often an *unbalanced* dataset, where the number of “negative” samples is much more than the number of “positive” samples, leading to an *inaccurate* classifier.

LSE-based classifier. Our idea is that we attempt to obtain more “positive” training samples and develop a classification rule. First, we initialize a training set \mathcal{R}_t by randomly sampling t distortion levels $[c_1, \dots, c_t]$ and computing their function values $\mathbf{f}_{1:t} = [f(c_1), \dots, f(c_t)]$, where t is a small number. Second, we use \mathcal{R}_t to learn a Gaussian process (GP) [26] to approximate f . We assume that f is a smooth function drawn from a GP, i.e. $f(c) \sim \text{GP}(m(c), k(c, c'))$, where $m(c)$ and $k(c, c')$ are the mean and covariance functions. We compute the *predictive distribution* for $f(c)$ at any point c as a Gaussian distribution, with its mean and

variance functions:

$$\mu_t(c) = \mathbf{k}^\top K^{-1} \mathbf{f}_{1:t} \quad (1)$$

$$\sigma_t^2(c) = k(c, c) - \mathbf{k}^\top K^{-1} \mathbf{k} \quad (2)$$

where \mathbf{k} is a vector with its i -th element defined as $k(c_i, c)$ and K is a matrix of size $t \times t$ with its (i, j) -th element defined as $k(c_i, c_j)$. Third, we iteratively update the training set \mathcal{R}_t by adding the new point $\{c_{t+1}, f(c_{t+1})\}$ until the sampling budget I is depleted, and at each iteration we update the GP. Instead of randomly sampling c_{t+1} , we maximize the acquisition function Straddle proposed in the LSE algorithm [5] to select c_{t+1} , which has the following form:

$$q(c) = 1.96 \times \sigma(c) - |\mu(c) - h|, \quad (3)$$

$$c_{t+1} = \underset{c \in \mathcal{C}}{\text{argmax}} q(c) \quad (4)$$

where $\mu(c)$ and $\sigma(c)$ are the predictive mean and standard deviation from Equations (1) and (2). Our sampling strategy achieves two goals: (1) sampling c where the model's accuracy is close to the threshold h (i.e. small $|\mu(c) - h|$) and (2) sampling c where the model's accuracy is highly uncertain (i.e. large $\sigma(c)$). As a result, we obtain more “positive” samples to train our GP. Finally, given any point $c \in \mathcal{C}$, as its predictive function value is between $\mu(c) - 2\sigma(c)$ and $\mu(c) + 2\sigma(c)$ with 95% probability, we form our classification rule as follow:

$$\text{label of } c = \begin{cases} 1, & \text{if } \mu(c) - 2\sigma(c) \geq h \\ 0, & \text{otherwise} \end{cases} \quad (5)$$

3.2. Model assurance with few images

We extend our method to the “few sample” setting where only few images are available in the assurance set. In other words, we acquire only few distorted images for the model evaluation. Our method has two steps: (1) we generate synthetic images and (2) we use both original and synthetic images in our LSE-based classifier.

3.2.1 Generating synthetic images

We develop a generative model based on CVAE [27]. We first review the “CVAE loss” used in the standard CVAE. We then describe our two new losses “distribution loss” and “prediction loss” to improve CVAE to generate high-quality and diverse images.

CVAE loss. CVAE aims to generate images similar to its real input images. Using the assurance set $\mathcal{D} = \{x_i, y_i\}_{i=1}^N$, CVAE trains encoder and decoder networks to learn a distribution of latent variable $z \in \mathbb{R}^l$. The encoder network maps an input image x along with its label y to the latent vector z that follows $P(z | y)$. The decoder network takes

z conditioned on y to reconstruct x . The standard loss to train CVAE is as follows:

$$\mathcal{L}_{cvae} = \mathcal{L}_{CE}(x, \tilde{x}) + \mathcal{L}_{KL}(Q(z | x, y), P(z | y)), \quad (6)$$

where $\mathcal{L}_{CE}(x, \tilde{x})$ is the cross-entropy loss between the original image x and the reconstructed image \tilde{x} and $\mathcal{L}_{KL}(Q(z | x, y), P(z | y))$ is a Kullback–Leibler divergence between the approximated posterior distribution of z and the prior distribution of z conditioned on y . We choose a Gaussian distribution for $P(z | y)$ i.e. $P(z | y) \equiv \mathcal{N}(0, I)$.

Distribution loss. Although CVAE can generate images, the diversity of generated images is quite limited as its training data \mathcal{D} is small. Thus, we encourage CVAE to generate more out-of-distribution images by adding a new *distribution loss* term. Our idea is that we match reconstructed images to the images in both \mathcal{D} and \mathcal{D}_T , where \mathcal{D} is the training images of CVAE and \mathcal{D}_T is the training images of the pre-trained deep model T (typically, $|\mathcal{D}_T| \gg |\mathcal{D}|$). Here, we cannot access \mathcal{D}_T since the model owner may not disclose their training data. Hence, we obtain the statistics of \mathcal{D}_T via the widely-used Batch-Norm (BN) layers in T . As a BN layer normalizes the feature maps during training to eliminate covariate shifts, it computes the channel-wise means and variances of feature maps [17, 34]. As a result, we try to minimize the distance between the feature statistics of reconstructed images and original images in \mathcal{D}_T . For each batch of reconstructed images $\{\tilde{x}_i\}_{i=1}^B$ (where B is the batch size), we put them into T to obtain their feature maps $\{a_i\}_{i=1}^B$ corresponding to the first convolution layer, and then compute the mean $\mu(\{a_i\}) = \frac{1}{B} \sum_{i=1}^B a_i$ and the variance $\sigma^2(\{a_i\}) = \frac{1}{B} \sum_{i=1}^B (a_i - \mu(\{a_i\}))^2$. We then extract the running-mean μ_{BN} and the running-variance σ_{BN}^2 stored in the first BN layer of T . Finally, we compute our distribution loss as:

$$\mathcal{L}_{dist} = \|\mu(\{a_i\}) - \mu_{BN}\|_2 + \|\sigma^2(\{a_i\}) - \sigma_{BN}^2\|_2, \quad (7)$$

where $\|\cdot\|_2$ is l_2 norm. We use the first BN layer since we want to match the low-level features of the images in \mathcal{D}_T , which are more task-agnostic. In contrast, higher BN layers capture high-level features that are more task-specific.

Prediction loss. Besides the diversity, the quality of generated images is also important. To this end, we introduce another loss term – *prediction loss*, which encourages the generated images look more natural. Remind that we reconstruct an image \tilde{x} using a latent vector z and a label y via the decoder network. If \tilde{x} is a random looking image and far from realistic, the model T cannot recognize \tilde{x} . In contrast, if \tilde{x} looks real, T should be able to predict a label \tilde{y} for \tilde{x} the same as y . For example, if the input image x is an image of “dog”, then y is “dog” and T should classify the reconstructed image \tilde{x} as “dog”. Based on this observation, we formulate our prediction loss:

$$\mathcal{L}_{pred} = \mathcal{L}_{CE}(y, T(\tilde{x})), \quad (8)$$

where $\mathcal{L}_{CE}(y, T(\tilde{x}))$ is the cross-entropy loss between the input label y and the softmax prediction of the model T for the reconstructed image \tilde{x} .

Final loss. We combine Equations (6), (7), (8) to derive the final loss to train our generative model:

$$\mathcal{L}_{final} = \mathcal{L}_{cvae} + \mathcal{L}_{dist} + \mathcal{L}_{pred} \quad (9)$$

After our generative model is trained, we can generate images via $G(z, y)$, where $z \sim \mathcal{N}(0, I)$, y is a label, and G is the trained decoder network.

Post-processing. As not all generated images have good visual quality, we implement a post-processing step to select the good ones. Assume that we generate M synthetic images $\hat{\mathcal{D}} = \{\hat{x}_1, \dots, \hat{x}_M\}$. We then use T to predict their class probabilities $O = \{T(\hat{x}_1), \dots, T(\hat{x}_M)\}$, and measure the confidence of T on the generated images. The confidence scores are computed as $E = \{e_1, \dots, e_M\}$, where $e_i = \max(T(\hat{x}_i))$. If the confidence score is high, the synthetic image looks more real as T confidently predicts the label. Finally, we select the synthetic images whose the confidence scores are greater than a *confidence level* α .

Our final set of synthetic images is computed as:

$$\hat{\mathcal{D}}_{final} = \{\hat{x}_i \in \hat{\mathcal{D}} \mid e_i > \alpha\} \quad (10)$$

3.2.2 Training our LSE-based classifier

We augment the set of synthetic images $\hat{\mathcal{D}}_{final}$ to the set of original images \mathcal{D} , and use $\mathcal{D} \cup \hat{\mathcal{D}}_{final}$ in our LSE-based classifier (as described earlier). With synthetic images, our classifier significantly improves its performance in the “few sample” setting as shown in our experiments.

4. Experiments and Discussions

We conduct comprehensive experiments to show that our method is better than other methods under both settings: *full set of images* and *few images*.

4.1. Experiment settings

4.1.1 Datasets

We use five image datasets MNIST, Fashion, CIFAR-10, CIFAR-100, and Tiny-ImageNet. They are commonly used to evaluate image classification methods [11, 24, 23].

4.1.2 Constructing the test set for the MAID problem

For each image dataset, we use its training set to train the model T and use its validation set for the assurance set \mathcal{D} in the MAID problem. Inspired by [8], we assure the model T against five image distortions as shown in Table 1. Note that our method is applicable to *any* distortion types as long as they can be defined by a range of values.

Table 1. List of distortions along with their domains.

Distortion	Domain	Description
Rotation	[0, 90]	Rotate 0° - 90°
Scale	[0.7, 1.3]	Zoom in/out 0-30%
Translation-X	[-0.2, 0.2]	Shift left/right 0-20%
Translation-Y	[-0.2, 0.2]	Shift up/down 0-20%
Brightness	[0.7, 1.3]	Darken/brighten 0-30%

To evaluate the performance of each assurance method, we need to construct the test set. Inspired by LSE methods [9, 10], we create a grid of data points in the search space (here, *each data point is a distortion level*). For each dimension, we use five points, resulting in 3,125 grid points in total. For each point c , we use it to modify the images in \mathcal{D} , and compute T 's accuracy on the set of distorted images \mathcal{D}'_c . If the accuracy is greater than a threshold, c is assigned a “positive” label. Otherwise, c has a “negative” label. At the end, there are 3,125 test points along with their labels. We report the numbers of “positive” and “negative” test points for each image dataset in Appendix 1.

4.1.3 Evaluation metric

We use each assurance method to predict labels for 3,125 test points and compare them with the true labels. Since the number of “positive” test points is much smaller than the number of “negative” test points, we use the F1-score (i.e. the harmonic mean of precision and recall) to evaluate the prediction. The higher the F1-score, the better in prediction.

4.1.4 Training the image classifier T

As most AI companies offer general AI-based services, it is reasonable to assume that the model developers do not know about the deployment conditions at the customer side. Thus, we use pre-trained models from [22] for T , which achieve similar accuracy on the original validation set as those reported in [29, 31, 2]. As pointed out by [18, 14, 20], we expect that these models will reduce their performance when evaluated on *unseen distorted images* (evidenced by the large number of “negative” test points). Note that our method can verify/assure *any* image classifiers.

4.1.5 Baselines

For the MAID problem (see Section 3.1), we compare our LSE-based classifier (called **LSE-C**) with five popular machine learning classifiers, including *decision tree* (DT), *random forest* (RF), *logistic regression* (LR), *support vector machine* (SVM), and *neural network* (NN). Since we are dealing with imbalanced classification, we modify the loss functions to allocate high/low weights for minority/majority samples using the inverse class frequency. This approach

called “*cost-sensitive learning*” [28]. We also compare with other well-known techniques to train a classifier with imbalanced data, including 2 under-sampling methods (*RandomUnder* and *NearMiss*), 3 over-sampling methods (*RandomOver*, *SMOTE*, and *AdaSyn*), and 2 generative methods (*GAN* and *VAE*). Their details are in [19, 25].

For MAID with few images (see Section 3.2), we compare our “few sample” version (called **FS-LSE-C**) with 3 baselines *CVAE-LSE-C*, *CGAN-LSE-C*, and *MixUp-LSE-C*. Similar to our method, these baselines first use CVAE [27], CGAN [21], or MixUp [13] to generate synthetic images, then apply LSE-C to both original and synthetic images. In this experiment, we want to show that our generative model is better than the other techniques for image generation, and helps towards better classification.

For a fair comparison, we use the same assurance set \mathcal{D} and sampling budget ($I = 400$) for all methods. In the “few image” setting, we generate the same number of synthetic images for all methods. We use the same network architecture and hyper-parameters for CVAE-LSE-C and our FS-LSE-C. The difference is that CVAE-LSE-C uses the standard CVAE loss in Equation (6) while FS-LSE-C uses our proposed loss in Equation (9). We use the confidence level $\alpha = 0.8$ to select qualified generated images across all experiments. We repeat each method three times with random seeds, and report its averaged F1-score. We do not report the standard deviations since they are small (< 0.02).

4.2. Results on MNIST and Fashion

The pre-trained image classifiers T achieve 99.31% and 92.67% accuracy on MNIST and Fashion (the accuracy is measured on the original validation set). We set the threshold $h = 95\%$ for MNIST and $h = 85\%$ for Fashion. Both datasets have 10 classes, and each class has 6K training images, and 1K testing images.

4.2.1 Results with the “full set of images” setting

We evaluate our method when the assurance set \mathcal{D} contains the full set of images (10K images). Table 2 shows that our method LSE-C is much better than other methods, where its improvements are around 7% (MNIST) and 30% (Fashion) over the best baseline. Note that as each imbalance handling technique is combined with 5 classifiers, we only report the best combination.

4.2.2 Results with the “few image” setting

We evaluate our method when the assurance set \mathcal{D} contains only few images (*5 images/class*). We train our generative model with feed-forward neural networks for encoder and decoder, latent dim = 2, batch size = 16, and #epochs = 600.

As shown in Table 3, all methods significantly drop their performance when run with few images. With synthetic im-

Table 2. F1-scores on MNIST and Fashion. “ N ” shows the number of original images used by each method.

Dataset	Method	N	F1-score
MNIST	Cost-Sensitive	10,000	0.6727
	RU	10,000	0.2118
	NearMiss	10,000	0.2789
	RO	10,000	0.6657
	SMOTE	10,000	0.6253
	AdaSyn	10,000	0.6322
	GAN	10,000	0.5687
	VAE	10,000	0.5952
	LSE-C (Ours)	10,000	0.7444
Fashion	Cost-Sensitive	10,000	0.3481
	RU	10,000	0.0078
	NearMiss	10,000	0.0078
	RO	10,000	0.3538
	SMOTE	10,000	0.3538
	AdaSyn	10,000	0.3538
	GAN	10,000	0.2169
	VAE	10,000	0.3481
	LSE-C (Ours)	10,000	0.6558

Table 3. F1-scores on MNIST and Fashion. “ N ” and “ M ” show the number of original and synthetic images used by each method.

Dataset	Method	N	M	F1-score
MNIST	AdaSyn	50	-	0.5771
	LSE-C (Ours)	50	-	0.5321
	CVAE-LSE-C	50	500	0.0417
	CGAN-LSE-C	50	500	0.0308
	MixUp-LSE-C	50	500	0.0923
	FS-LSE-C (Ours)	50	500	0.5951
Fashion	SMOTE	50	-	0.3446
	LSE-C (Ours)	50	-	0.4444
	CVAE-LSE-C	50	500	0.1481
	CGAN-LSE-C	50	500	0.0833
	MixUp-LSE-C	50	500	0.3846
	FS-LSE-C (Ours)	50	500	0.5808

ages, our “few sample” version FS-LSE-C greatly improves its F1-scores over LSE-C and other methods. Here, we only report F1-scores of AdaSyn and SMOTE (the best imbalance handling methods). Other results are in Appendix 2.

Other generative-based methods do not show any benefit, where their performance is much lower than ours. This is because their synthetic images do not have enough diversity as CVAE and CGAN easily over-fit and memorize few samples due to their limited training data (only 5 images/class).

4.3. Results on CIFAR-10 and CIFAR-100

The pre-trained image classifiers T achieve 91.37% accuracy on CIFAR-10 and 69.08% accuracy on CIFAR-100. We assure T with the thresholds $h = 85\%$ (CIFAR-10) and

$h = 65\%$ (CIFAR-100). CIFAR-10 contains RGB images with 10 classes, and each class has 5K training and 1K testing images. CIFAR-100 has 100 classes, and each of them has 500 training and 100 testing images.

4.3.1 Results with the “full set of images” setting

From Table 4, our method LSE-C is the best method, where its improvements are notable. Cost-Sen is generally better than other methods. Over-sampling and generative methods always outperform under-sampling methods.

Note that instead of using random points, we can use the points suggested by Equation (4) to train a machine learning classifier. We compare with this approach in Appendix 3.

Table 4. F1-scores on CIFAR in the “full set of images” setting.

Dataset	Method	N	F1-score
CIFAR-10	Cost-Sensitive	10,000	0.8549
	RU	10,000	0.7524
	NearMiss	10,000	0.7923
	RO	10,000	0.8489
	SMOTE	10,000	0.8570
	AdaSyn	10,000	0.8563
	GAN	10,000	0.8551
	VAE	10,000	0.8567
		LSE-C (Ours)	10,000
CIFAR-100	Cost-Sensitive	10,000	0.7115
	RU	10,000	0.2016
	NearMiss	10,000	0.2246
	RO	10,000	0.7115
	SMOTE	10,000	0.5540
	AdaSyn	10,000	0.5538
	GAN	10,000	0.6207
	VAE	10,000	0.5751
		LSE-C (Ours)	10,000

Table 5. F1-scores on CIFAR in the “few image” setting.

Dataset	Method	N	M	F1-score
CIFAR-10	AdaSyn	50	-	0.7901
	LSE-C (Ours)	50	-	0.8128
	CVAE-LSE-C	50	500	0.0090
	CGAN-LSE-C	50	500	0.0089
	MixUp-LSE-C	50	500	0.8697
	FS-LSE-C (Ours)	50	500	0.8687
CIFAR-100	RO	500	-	0.2788
	LSE-C (Ours)	500	-	0.3010
	CVAE-LSE-C	500	500	0.0000
	CGAN-LSE-C	500	500	0.0000
	MixUp-LSE-C	500	500	0.4094
	FS-LSE-C (Ours)	500	500	0.5787

4.3.2 Results with the “few image” setting

We train our CVAE with convolutional neural networks for both encoder and decoder, with latent dimension = 2, batch size = 64, and #epochs = 600.

From Table 5, our FS-LSE-C is much better than other generative methods. It is comparable with MixUp-LSE-C on CIFAR-10 but much better on CIFAR-100. As expected, our LSE-C drops its F1-score when run with few images, but it still outperforms over-sampling methods ~2-3%.

4.4. Results on Tiny-ImageNet

For the “full set of images” setting (Table 6), our LSE-C achieves 0.9113 F1-score, which is much better than the best baseline RO (0.7453). For the “few image” setting, our FS-LSE-C becomes the best, where its F1-score is 0.8287 vs. MixUp-LSE-C (0.6938). Details are in Appendix 4.

Table 6. F1-scores on Tiny-IN in the “full set of images” setting.

Dataset	Method	N	F1-score
Tiny-IN	Cost-Sensitive	10,000	0.7053
	RU	10,000	0.4207
	NearMiss	10,000	0.5014
	RO	10,000	0.7453
	SMOTE	10,000	0.7267
	AdaSyn	10,000	0.7385
	GAN	10,000	0.6687
	VAE	10,000	0.6635
	LSE-C (Ours)	10,000	0.9113

The results in Tables 2-6 suggest that our methods are effective under both settings and always better than existing methods. With our novel generative model to synthesize images, our methods solve the model assurance problem more efficient and realistic even with only few images.

4.5. Ablation study

We conduct further experiments on CIFAR-10 to analyze our method FS-LSE-C under the “few image” setting.

4.5.1 Different types of components

Compared to the standard CVAE, our generative model has three new components: *distribution loss*, *prediction loss*, and *post-processing step*. Table 7 reports the F1-score of each component. While CVAE-LSE-C using CVAE alone only achieves 0.0090, each individual component in our method (except the prediction loss) shows a significant improvement. The post-processing becomes the most successful component, achieving up to 0.7546. By combining the post-processing with the prediction loss or the distribution loss, our method further improves its F1-score up to 0.8132 and 0.8223 respectively. Finally, when using all three components together, we achieve the best result at 0.8687.

Figure 2 shows synthetic images generated by CVAE and our generative model with different losses. The CVAE images are often unclear due to its limited training data. With our prediction and distribution losses, the synthetic images are slightly better. Our final generative model generates the best-quality images, where the subjects (e.g. “dog”, “cat”) are clearly recognized and visualized.

FID scores. We compute the Frechet inception distance (FID) scores [12] to measure the quality of the generated images (lower is better): CVAE (6.99), PRED loss (7.56), DIST loss (5.57), and our generative model (4.36).

The ablation study suggests that each component in our generative model is useful, which greatly improves the classification performance compared to the standard CVAE. By combining all three components, our generative model generates high-quality and diverse synthetic images.

4.5.2 Hyper-parameter analysis

There is one important hyper-parameter in our framework, which is the confidence level $\alpha \in [0, 1]$ to select good generated images in the post-processing step. We investigate how the different values of α affect our F1-score.

From Figure 3, our “few sample” version FS-LSE-C is always better than LSE-C with $\alpha \in [0.75, 0.95]$. More importantly, it is stable with a large range of α values, where its F1-score is just slightly changed. When α is small (i.e. $\alpha < 0.75$), it may drop its F1-score as most of generated images are not confidently recognized. When α is too large (i.e. $\alpha > 0.95$), it also reduces its F1-score since very few synthetic images are generated under this strict constraint.

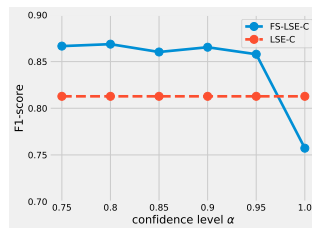


Figure 3. F1-score vs. confidence level α on CIFAR-10.

4.5.3 Numbers of original and synthetic images

We investigate the effect of the number of original and generated images on our method’s performance in Appendix 5.

In summary, both methods LSE-C and FS-LSE-C are improved with more original images. FS-LSE-C is improved with more synthetic images and is always better than LSE-C (our version does not use synthetic images).

4.5.4 Visualization

We visualize the “positive” and “negative” points classified by our methods using t-SNE [30], and compare them with

Table 7. Effectiveness of different components in our method FS-LSE-C.

	CVAE-LSE-C	FS-LSE-C (Ours)						
Distribution loss		✓			✓	✓		✓
Prediction loss			✓		✓		✓	✓
Post-processing				✓		✓	✓	✓
F1-score	0.0090	0.1079	0.0090	0.7546	0.4652	0.8223	0.8132	0.8687

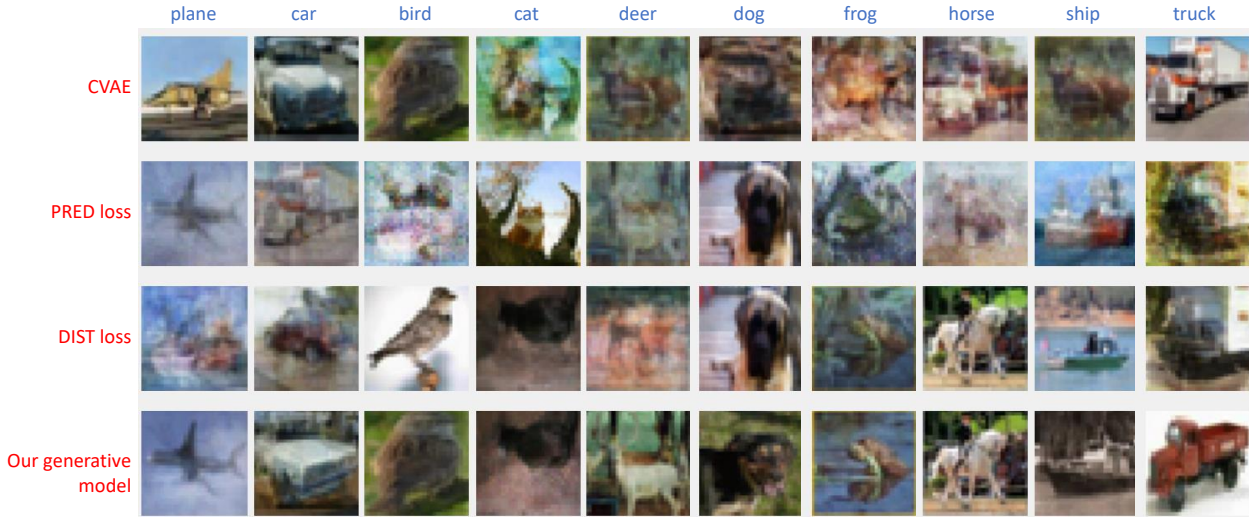


Figure 2. Synthetic images generated by CVAE and our generative model with different losses. “PRED loss” and “DIST loss” mean our model only uses the prediction loss (Eq. (8)) or the distribution loss (Eq. (7)). The text on the top indicates the labels of generated images.

the ground-truth labels in Figure 4. In summary, our methods correctly predict the labels for the test points.

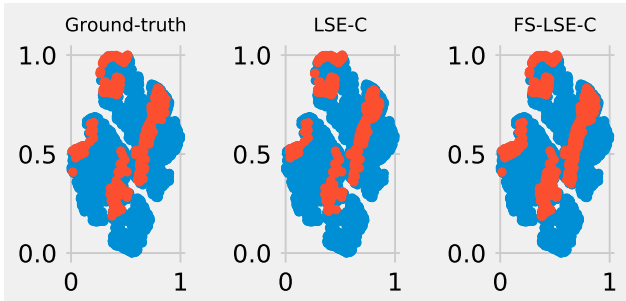


Figure 4. “Positive” and “negative” points classified by our methods vs. the ground-truth on CIFAR-10. Red dots denote “positive” points while blue dots denote “negative” points.

5. Conclusion

We address the problem *Model Assurance under Image Distortion* (MAID) i.e. we seek to find all distortion levels where the accuracy of a pre-trained deep model exceeds a threshold. By doing this, we gain knowledge of the model’s strengths and weaknesses before deploying it in real-world. Since MAID can be formed as a classification task, we proposed a novel classifier based on a LSE algorithm. Our idea is to approximate the expensive, black-box function map-

ping from a distortion level to the model’s accuracy on distorted images using GP. We then leverage the GP’s mean and variance to form our classification rule.

We further extend our method to a “few sample” setting where we can acquire only few real images to perform the model assurance process. We develop a CVAE-based generative model, with two new loss functions and a post-processing step. These components allow our generative model to produce a high-quality and diverse synthetic images, which significantly improves the performance of our LSE-based classifier. Our method does not require many labeled samples, thus it can be directly applied to domains where labeled images are difficult to collect e.g. medical or satellite images. We demonstrate the benefits of our methods on five image datasets, where they greatly outperform other methods including machine learning classifiers with imbalance handling capability and generative methods.

References

- [1] Namhyuk Ahn, Byungkon Kang, and Kyung-Ah Sohn. Image distortion detection using convolutional neural network. In *IEEE Asian Conference on Pattern Recognition (ACPR)*, pages 220–225, 2017. 2
- [2] Prashant Bhat, Elahe Arani, and Bahram Zonooz. Distill on the go: Online knowledge distillation in self-

- supervised learning. In *CVPR*, pages 2678–2687, 2021. 5
- [3] Ilija Bogunovic, Jonathan Scarlett, Andreas Krause, and Volkan Cevher. Truncated variance reduction: A unified approach to bayesian optimization and level-set estimation. *NIPS*, 29, 2016. 2
- [4] Sebastian Bosse, Dominique Maniry, Thomas Wiegand, and Wojciech Samek. A deep neural network for image quality assessment. In *IEEE International Conference on Image Processing (ICIP)*, pages 3773–3777, 2016. 2
- [5] Brent Bryan, Robert Nichol, Christopher Genovese, Jeff Schneider, Christopher Miller, and Larry Wasserman. Active learning for identifying function threshold boundaries. *NIPS*, 18, 2005. 2, 3
- [6] Brent Bryan and Jeff Schneider. Actively learning level-sets of composite functions. In *ICML*, pages 80–87, 2008. 2
- [7] Samuel Dodge and Lina Karam. Quality robust mixtures of deep neural networks. *IEEE Transactions on Image Processing*, 27(11):5553–5562, 2018. 2
- [8] Shivapratap Gopakumar, Sunil Gupta, Santu Rana, Vu Nguyen, and Svetha Venkatesh. Algorithmic assurance: An active approach to algorithmic testing using bayesian optimisation. In *NIPS*, pages 5466–5474, 2018. 2, 4
- [9] Alkis Gotovos, Nathalie Casati, Gregory Hitz, and Andreas Krause. Active learning for level set estimation. In *IJCAI*, pages 1344–1350, 2013. 2, 5
- [10] Huong Ha, Sunil Gupta, Santu Rana, and Svetha Venkatesh. High Dimensional Level Set Estimation with Bayesian Neural Network. In *AAAI*, volume 35, pages 12095–12103, 2021. 2, 5
- [11] Kaiming He, Xiangyu Zhang, Shaoqing Ren, and Jian Sun. Deep residual learning for image recognition. In *CVPR*, pages 770–778, 2016. 1, 4
- [12] Martin Heusel, Hubert Ramsauer, Thomas Unterthiner, Bernhard Nessler, and Sepp Hochreiter. Gans trained by a two time-scale update rule converge to a local nash equilibrium. *NIPS*, 30, 2017. 7
- [13] Zhang Hongyi, Cisse Moustapha, Dauphin Yann, and Lopez-Paz David. mixup: Beyond empirical risk minimization. In *ICLR*, 2018. 5
- [14] Md Tahmid Hossain, Shyh Wei Teng, Dengsheng Zhang, Suryani Lim, and Guojun Lu. Distortion robust image classification using deep convolutional neural network with discrete cosine transform. In *IEEE International Conference on Image Processing (ICIP)*, pages 659–663, 2019. 2, 5
- [15] Yu Inatsu, Masayuki Karasuyama, Keiichi Inoue, and Ichiro Takeuchi. Active learning for level set estimation under cost-dependent input uncertainty. *arXiv preprint arXiv:1909.06064*, 2019. 2
- [16] Yu Inatsu, Masayuki Karasuyama, Keiichi Inoue, and Ichiro Takeuchi. Active learning for level set estimation under input uncertainty and its extensions. *Neural Computation*, 32(12):2486–2531, 2020. 2
- [17] Sergey Ioffe and Christian Szegedy. Batch normalization: Accelerating deep network training by reducing internal covariate shift. In *ICML*, pages 448–456, 2015. 4
- [18] Le Kang, Peng Ye, Yi Li, and David Doermann. Convolutional neural networks for no-reference image quality assessment. In *CVPR*, pages 1733–1740, 2014. 2, 5
- [19] Joffrey Leevy, Taghi Khoshgoftaar, Richard A Bauder, and Naeem Seliya. A survey on addressing high-class imbalance in big data. *Journal of Big Data*, 5(1):1–30, 2018. 5
- [20] Xiaoyu Li, Bo Zhang, Pedro Sander, and Jing Liao. Blind geometric distortion correction on images through deep learning. In *CVPR*, pages 4855–4864, 2019. 1, 2, 5
- [21] Mehdi Mirza and Simon Osindero. Conditional generative adversarial nets. *arXiv preprint arXiv:1411.1784*, 2014. 3, 5
- [22] Dang Nguyen, Sunil Gupta, Kien Do, and Svetha Venkatesh. Black-box few-shot knowledge distillation. In *ECCV*, 2022. 5
- [23] Dang Nguyen, Sunil Gupta, Trong Nguyen, Santu Rana, Phuoc Nguyen, Truyen Tran, Ky Le, Shannon Ryan, and Svetha Venkatesh. Knowledge distillation with distribution mismatch. In *ECML-PKDD*, pages 250–265, 2021. 4
- [24] Waseem Rawat and Zenghui Wang. Deep convolutional neural networks for image classification: A comprehensive review. *Neural Computation*, 29(9):2352–2449, 2017. 4
- [25] Vignesh Sampath, Iñaki Murtua, Juan Jose Aguilar Martin, and Aitor Gutierrez. A survey on generative adversarial networks for imbalance problems in computer vision tasks. *Journal of Big Data*, 8:1–59, 2021. 5
- [26] Jasper Snoek, Hugo Larochelle, and Ryan Adams. Practical Bayesian optimization of machine learning algorithms. In *NIPS*, pages 2951–2959, 2012. 2, 3
- [27] Kihyuk Sohn, Honglak Lee, and Xinchen Yan. Learning structured output representation using deep conditional generative models. *NIPS*, pages 3483–3491, 2015. 2, 3, 5

- [28] Nguyen Thai-Nghe, Zeno Gantner, and Lars Schmidt-Thieme. Cost-sensitive learning methods for imbalanced data. In *IJCNN*, pages 1–8, 2010. 5
- [29] Yonglong Tian, Dilip Krishnan, and Phillip Isola. Contrastive representation distillation. In *ICLR*, 2020. 5
- [30] Laurens Van der Maaten and Geoffrey Hinton. Visualizing data using t-SNE. *Journal of Machine Learning Research*, 9(11):2579–2605, 2008. 7
- [31] Dongdong Wang, Yandong Li, Liqiang Wang, and Boqing Gong. Neural Networks Are More Productive Teachers Than Human Raters: Active Mixup for Data-Efficient Knowledge Distillation from a Black-box Model. In *CVPR*, pages 1498–1507, 2020. 3, 5
- [32] Yaqing Wang, Quanming Yao, James Kwok, and Lionel Ni. Generalizing from a few examples: A survey on few-shot learning. *ACM Computing Surveys*, 53(3):1–34, 2020. 3
- [33] Jingyi Xu and Hieu Le. Generating representative samples for few-shot classification. In *CVPR*, pages 9003–9013, 2022. 3
- [34] Hongxu Yin, Pavlo Molchanov, Jose Alvarez, Zhizhong Li, Arun Mallya, Derek Hoiem, Niraj Jha, and Jan Kautz. Dreaming to distill: Data-free knowledge transfer via DeepInversion. In *CVPR*, pages 8715–8724, 2020. 4
- [35] Yiren Zhou, Sibong Song, and Ngai-Man Cheung. On classification of distorted images with deep convolutional neural networks. In *IEEE International Conference on Acoustics, Speech and Signal Processing (ICASSP)*, pages 1213–1217, 2017. 2